

# Generation of Added Values Products Supporting Risk Analysis

Massimo Musacchio et al.\*

*Istituto Nazionale di Geofisica e Vulcanologia, Rome  
Italy*

## 1. Introduction

Active volcanoes are spread all over the world and are located in specific areas correlated to geologic structures. In the last 10,000 years more than 1300 volcanoes have erupted, but only half of the eruptions have been reported in historical texts. It has been estimated that every year 50 volcanic eruption may occur threatening about 10 % of the worldwide population. Considering the constant increase in human population and that many major cities are placed in the proximity of active volcanoes, the number of people subjected to the risks caused by volcanic eruptions is also increasing. Stated the problem dimension, it shall be defined the method to counter act the crisis scenario. A volcanic eruption can be faced under different point of view, on one side it can be deeply studied in order to improve the knowledge of geophysical mechanism which drives the eruption itself, on the other hand it is important to set up a service based on the integration of different dataset and aimed to deliver added values products toward those who are in charge to manage the risk associated. One response to last sentence is the Sistema Rischio Vulcanico (ASI-SRV) project funded by the Italian Space Agency (ASI) in the frame of the National Space Plan 2003-2005 under the Earth Observations section for natural risks management. The ASI-SRV Project is coordinated by the Istituto Nazionale di Geofisica e Vulcanologia (INGV) which is responsible, in Italy, at national level for the volcanic monitoring. The main goal of the ASI-SRV project is to define, develop and demonstrate tools and products, based on the integration Earth Observation data (EO) with data coming from the ground monitoring network developed at national and local level, to support the risk management decision procedures. The project philosophy is to implement, by incremental versions, specific modules which allow to process, store and visualize through a dedicated Web-GIS tools, added value information derived by EO and No EO data.

---

\* Malvina Silvestri<sup>1</sup>, Luca Merucci<sup>1</sup>, Stefano Corradini<sup>1</sup>, Claudia Spinetti<sup>1</sup>, Valerio Lombardo<sup>1</sup>, Boris Behncke<sup>1</sup>, Lorenzo Guerrieri<sup>3</sup>, Gabriele Gangale<sup>3</sup>, Fabrizia Buongiorno<sup>1</sup>, Sergio Perelli<sup>2</sup>, Sergio Teggi<sup>3</sup>, Sergio Pugnaghi<sup>3</sup>, Angelo Amodio<sup>4</sup>, Eugenio Sansosti<sup>5</sup>, Simona Zoffoli<sup>6</sup> and Chiara Cardaci<sup>7</sup>

<sup>1</sup>Istituto Nazionale di Geofisica e Vulcanologia, Rome, Italy

<sup>2</sup>Advanced Computer System S.p.A, Rome

<sup>3</sup>Università degli Studi di Modena e Reggio Emilia, Modena,

<sup>4</sup>Galileian plus, via Vito Giuseppe Galati Rome,

<sup>5</sup>Istituto per il Rilevamento Elettromagnetico dell'Ambiente-CNR, Naples,

<sup>6</sup>Agenzia Spaziale Italiana, Agenzia Spaziale Italiana, Rome

<sup>7</sup>Dipartimento della Protezione Civile Rome, Italy

## 2. Rationale and goals

The “Volcanic Risk System (ASI-SRV)” is a three year (2007-2010) project, funded by the Italian Space Agency (ASI), aimed at defining, developing and demonstrating (at a pre-operational stage) a set of functionalities in support of a decisional system for volcanic risk management based on the use of Earth Observation (EO) data. Moreover, this pilot project supports research activities to fill in the gaps between the user needs and the available technology. The Civil Protection organism represents the National Authority which will get benefit from the space technology derived products for Volcanic Risk management and monitoring. During the project lifetime a great effort was dedicated to understand the organization of Department of the Civil Protection (DPC) in order to get specific requirements for services and products to be developed in this pre-operational project taking into account that the DPC is a division of the Italian Presidenza del Consiglio dei Ministri, and represents the national authority charged for civil protection activity; It addresses and coordinates all the forces operating on the Italian territory, during the emergency phases through the National warning system provided by DCP and Regions by the Functional Centres National Network. The main purpose of CFRV is to collect, share and synthesize data related to volcanic hazard provided by the monitoring centres (e.g. INGV). Functional Centres are the operative support units, which are able to collect, elaborate and exchange every kind of data provided from Competence Centres. These are Institutions which provide services, information, data, elaboration, technical and scientific contributions for specific topics.

During the volcanic emergency phases the functional centres for volcanic risk is supported by Synthesis Group. This group includes volcanologist of the High Risks Committee, the researchers of Competence Centre involved in the monitoring activities and a civil protection manager/officer expert in the risk evaluation. The Office “General Direction of Prevision, Evaluation, Prevention and Mitigation of Natural Risks” takes part in many European projects and participated in civil protection interventions in foreign countries. Operative Centre for Volcanic Risk is the scientific decision-support section of the DPC. For that reasons the End User is the Italian Department for Civil Protection (DPC).

The ASI-SRV system and products have been defined through a detailed User requirement survey that has been started in the Feasibility Study, funded by ASI in 2004 and integrated with information acquired in other project such as FP6-PREVIEW (2005-2008). The system architecture is based on different modules that could be activated depending of the Volcanic Phase (figure 1) addressed by the Italian Civil Protection Department (DPC):

- Early Warning (Knowledge and Prevention)
- Crisis
- Post-Crisis

Moreover the system is able to add new modules in order to have the flexibility to improve its performance by using new algorithms or new sensors. ASI-SRV has developed, in its final version, a centralized HW-SW system located at INGV which will control two complete processing chains, one located at INGV for Optical data, and the other located at CNR-IREA for SAR data. The produced results will be disseminated through a Web-GIS interface which will allow the End User to overview and assimilate the products in a compatible format respect to local monitoring needs in order to have an immediate use of the provided information.



Fig. 1. Synthetic risk cycle diagram

The ASI-SRV project has developed data processing modules dedicated to the generation of specific products meeting the user needs and to the dissemination of the information by means of dedicated Web-GIS. ASI-SRV system provides the capability to manage the import many different EO data into the system, it maintains a repository where the acquired data are stored and generates selected products which are functional to the phases described above. All technical choices and development of ASI-SRV are based on flexible and scalable modules which will take into account also the new coming space sensors, new processing algorithms considering the national and international scenario in the space technologies. An important step of the project development regards the technical and scientific feasibility of the provided products. In fact the technical feasibility depends on the data availability, accuracy algorithms and models used in the processing and of course the possibility to validate the results by means of comparison with other independent measurements (EO and non-EO). Archived series and near real time (NRT) acquisition of EO optical and radar data are used to derive information on surface and plume characteristics building the knowledge for the two volcanic systems composing the test sites, respectively Etna and Vesuvio Campi Flegrei. Considering the different type of volcanic activities characterizing the investigated volcanic complexes, different stacks of products type are necessary to the User considering also the product feasibility. Each product is generated by a specific modules based on algorithm developed by the researcher during last decade. All these modules can process in parallel EO optical data generating huge volume of products to be stored in the ASI-SRV main database, building a very long catalogue of geophysical parameters suitable for back analysis but also for better understand a complicate natural system as a volcano is. The generated and delivered products are divided according to the following paradigm: before a crisis, in order to recognize small variation of any geophysical parameter, high spatial resolution sensors have to be used, whilst during a crisis, in order to daily follow the ongoing eruption, sensors characterized by multi-acquisition per day are necessary. According to the sentence stated above the following products with respect to the test site have been chosen and generated:

Moreover the system is able to add new modules in order to have the flexibility to improve its performance by using new algorithms or new sensors. ASI-SRV has developed, in its final version, a centralized HW-SW system located at INGV which will control two complete processing chains, one located at INGV for Optical data, and the other located at

CNR-IREA for SAR data. The produced results will be disseminated through a Web-GIS interface which will allow the End User to overview and assimilate the products in a compatible format respect to local monitoring needs in order to have an immediate use of the provided information.

Phase	Product	Test Site
Early Warning	Multi-parametric Analysis	Mt.Etna, Vesuvio – Campi Flegrei
	Ground deformation velocity map and time series based on radar data	Mt.Etna and Vesuvio – Campi Flegrei
	Temperature Map, Thermal Flux	Mt.Etna, Campi Flegrei
	SO2 Columnar, Water Vapour Columnar Content, AOT Concentration map	Mt.Etna
Crisis	Deformation Map based on radar data	Mt.Etna
	Ground deformation velocity map and time series based on radar data	Mt.Etna
	Temperature Map, Thermal Flux, Effusion Rate	Mt.Etna
	SO2 Columnar Content and flux, Water Vapour Columnar Content, AOT Concentration map	Mt.Etna
Post Crisis	Ground deformation velocity map and time series based on radar data	Mt.Etna and Vesuvio – Campi Flegrei
	Lava thickness	Mt.Etna
	Ash distribution map Lava distribution map	Mt. Etna

Table 1. List of the products generated and delivered within ASI-SRV project. The background color is coherent with the risk phase indicating in figure 1

Moreover the system is able to add new modules in order to have the flexibility to improve its performance by using new algorithms or new sensors. ASI-SRV has developed, in its final version, a centralized HW-SW system located at INGV which will control two complete processing chains, one located at INGV for Optical data, and the other located at CNR-IREA for SAR data. The produced results will be disseminated through a Web-GIS interface which will allow the End User to overview and assimilate the products in a compatible format respect to local monitoring needs in order to have an immediate use of the provided information.

### 3. Processing chain

The ASI-SRV system has been thought as a semi-automatic system able to operate in unsupervised mode for all the modules where the human interaction is useless. It doesn't imply that the scientists role is negligible on the contrary this method will allow to gain time to spent in the processing and validation processes.

These "unsupervised" modules concern the automatic calibration, georeferencing, mosaiking, atmospheric and topographic correction. These modules start with the radiometric calibration, cut and mosaiking and atmospheric correction tool [1,2] and after the core data processes represented by scientific algorithm dedicated to the extraction of added value products and end with the publication of the vector layer via GIS Tool Analyst (GTA) via a dedicated MMI. The selected products (table 1) after the feasibility study have been transformed to functional requirements of the system. On the base of the functional requirements the system will have the following main sub-systems (Figure 2)

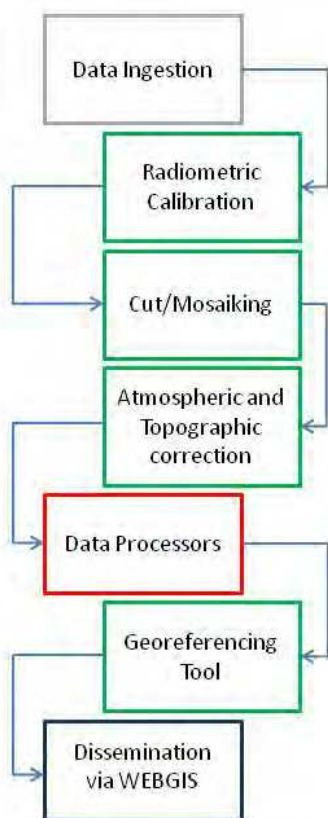


Fig. 2. ASI-SRV end to end processing flow; green boxes contain „general purposes“ module (which are remote sensed data independent), red box contains the core of the ASI-SRV system (module based on the integration of scientific alghorithm), dark blue box represents the Web-GIS interface.

All data are ingested into ASI-SRV system and are available to the processing functionality installed into main ASI-SRV Infrastructure. This system has been developed enabling the ingestion of different EO data sensors that can be processed contemporaneously. This processing chain requires that the ASI-SRV system is able to run in parallel allocating more than one parallel instances. One of the aim of the GP modules is to prepare the EO data in a specific file format including all attributes needed by each different processors and then the publication of the results. Considering that ASI-SRV architecture is based on a distributed and scalable client/server architecture this imply that different processors need to ingest data set characterized by a constant and common structure.

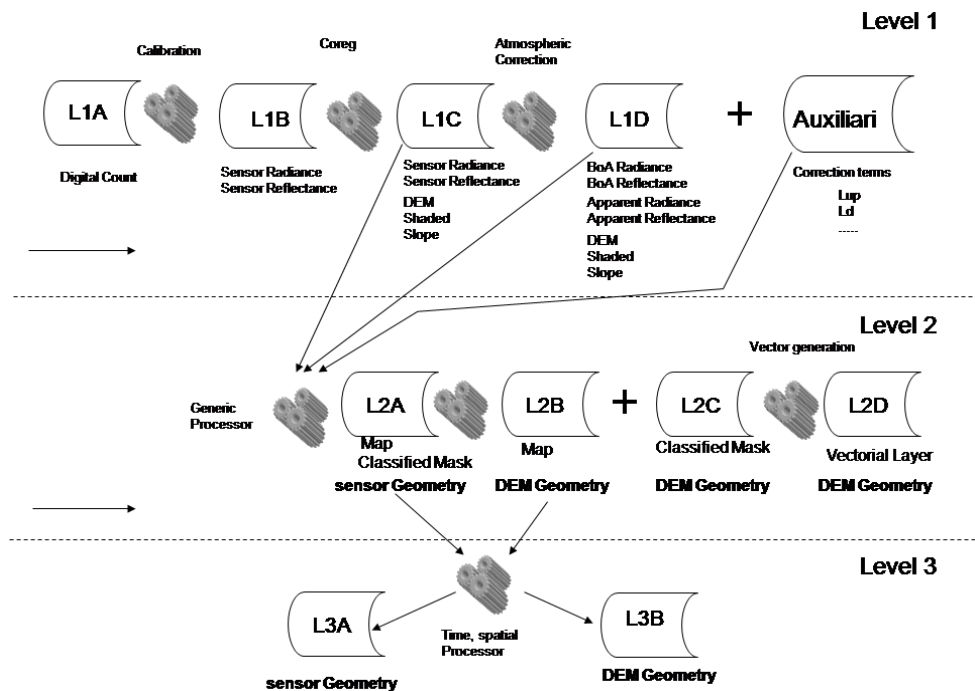


Fig. 3. ASI-SRV production chain. The General Purpose modules are dedicated to the production of all Level 1 dataset

The ASI-SRV production chain produce three level of product and the GP module is dedicated to the generation of all the L1 and to the L2D products (Figure 3). In the ASI-SRV project the EO data used have been classified with different level depending on the information contained. The level definition of processing is inspired to the CEOS standard (1992) with few differences. The definitions are the following:

- Level 1A: ingested data derived from the spaceborne. They do not contain information on calibration
- Level 1B calibrated data containing radiance/reflectance measured at the sensor
- Level 1C spatial resizing on the geographical windows; on these data DEM, Shaded Relief, Slope and Aspect are contained

- Level 1D equivalent to 1C level but containing the bottom of atmosphere radiance/reflectance and the apparent reflectance obtained using coefficients computed by atmospheric correction module
- Level 2A raster products; they contains geographical variables in the sensor geometry. Typically they can be divided in: :
  - A-1 containing the output derived from the processor module (i.e. map with results of algorithm implemented in the processing module)
  - A-2 containing the classified results according to criteria defined by the responsible of processing module
- Level 2B raster products equal to 2A-1 products projected in DEM geometry
- Level 2C raster products equal to 2A-2 products projected in DEM geometry
- Level 2D products in vector format (lines, curves, points) obtained using level 2C products
- Level 3 products obtained combining two or more products of level 2 resampled/processed in the space and time.

According to this level of classification each different step is represented by an HDF file format containing increased scientific dataset (Figure 3) with respect to the former.

#### 4. Test sites

According to the necessity of the Users and with the objectives of demonstrate the suitability of the defined products three different test sites have been chosen, two test sites are located in the Napoli Bay area (Mt. Vesuvius volcano and the Campi Flegrei Caldera) and one in Sicily, near Catania (Mt. Etna) (Figure 4). Those areas are characterized by different volcanic activity and surface phenomena enabling the capability to analyze the geophysical parameters useful to investigate the pre-crisis (early warning) the crisis and post crisis phases.

These three test sites have been selected by considering the present state of the volcanic activity and therefore ensure the demonstration of the selected products for each phase (Early Warning, Crisis and Post Crisis). Moreover second parameter used to selected the test areas has been the observability by space of the different volcanic phenomena. Mt. Etna volcano is characterized by an almost persistent volcanic activity, allowing the generation of products related to the sin-eruptive and post-eruptive phase. For this volcano it is possible to provide products also if no eruptive events have occurred, using EO data acquired during the eruptive events in the last years. Vesuvio and Campi Flegrei volcanoes are representative to quiescent phase products analysis, especially regarding the surface deformation map. Moreover the sites selection is compatible with the spatial resolution of EO operative systems and the frequent monitoring with ground networks permits the system to validate and integrate EO products

##### Etna test site

Mount Etna is Europe's largest volcano (its volume is at least 350 km<sup>3</sup>), and one of the most active (in the sense of "productive" and eruption frequency) volcanoes on Earth, with frequent periods of intermittent to persistent activity in the summit area and major eruptions from new vents on its flanks every 1-20 years. The main feature of Etnean activity is voluminous lava emission, but strong explosive activity occurs occasionally, mostly from its presently four summit craters. Some of the eruptions from its flanks also show high

degrees of explosivity, such as those in 1669, 1879, and 2002-2003. Etna lies near the eastern (Ionian) coast of Sicily and occupies a surface area of around 1200 km<sup>2</sup> with a perimeter exceeding 135 km. Its summit height varies frequently in function of eruptive activity or minor collapse events at the summit craters: through the early 1980s it showed a net increase by nearly 100 m to an unprecedented 3350 m in 1981. This growth was concentrated at the Northeast Crater, a feature that was born in 1911; nearly constant activity at this crater since the mid-1950s lead to the growth of a large cone around it. Activity of the Northeast Crater became rather infrequent since the mid-1980s, and since then the height of its cone has decreased to 3330 m as of 2007. The cone of the youngest of the four summit craters, the Southeast Crater, which was born in 1971, underwent a period of dramatic growth between 1998 and 2001 but remained 40 lower than the highest point at the summit, the Northeast Crater. Etna is particular for a number of reasons. First, it has the longest record of historical eruptions (see *Volcanoes of the World*, 1994 edition) among all volcanoes on this planet, its first historically documented eruption occurring at about 1500 BC. The total number of eruptions is 209 (18 among them questionable) through late 1993 (*Volcanoes of the World*). To these, there have now to be added the spectacular and vigorous summit eruptions of 1995-2001, the flank eruptions of 2001, 2002-2003, 2004-2005, and 2008-2009, plus a period of intermittent summit activity in 2006-2008. Certainly we will not have to wait long to add yet more eruptions, either at the summit or somewhere on the flanks, to this impressive record.

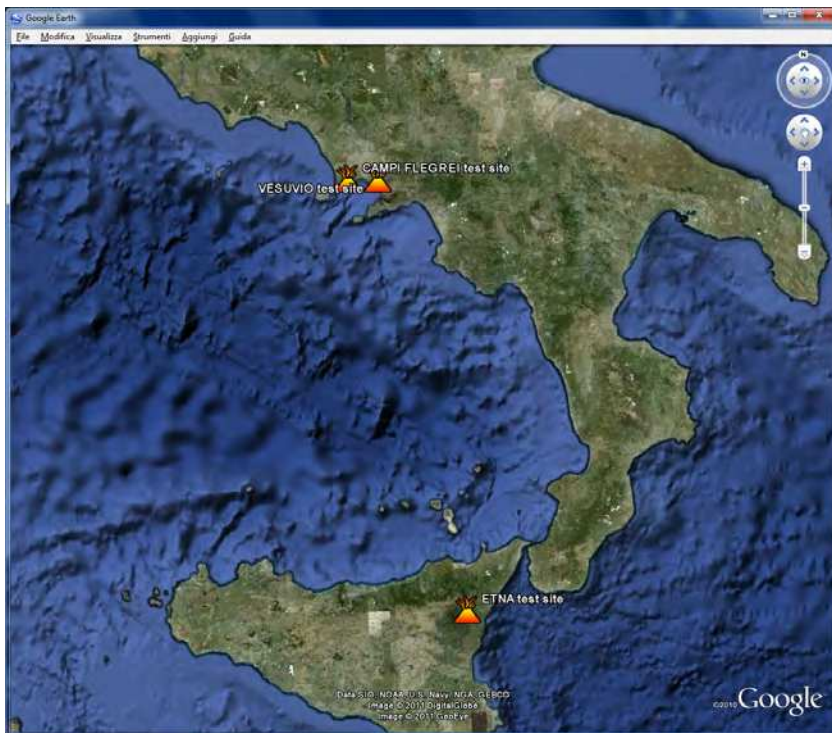


Fig. 4. Localization of the project test sites, from North to South Campi Flegrei, Veuvio and Etna respective (from Google Earth)



Etna lies in an area that is still not well understood from a geological standpoint. While some scientists relate, in a broader sense, the Etnan volcanism to subduction of the Ionian oceanic seafloor beneath the Calabrian Arc (with volcanism on the Aeolian Islands as one consequence), others postulate a hot spot beneath Etna, thus explaining its high lava production and fluid mafic magmas. Still another hypothesis sees Etna in a complex rifting environment, due to the inhomogeneous nature of convergence between the African and Eurasian plates with subduction of the oceanic Ionian sea floor underneath the Calabrian Arc, and much lower convergence rates on Sicily where both colliding margins are continental lithosphere. Among the few things which are quite well understood is the fact that the volcano lies at the intersection of several major regional fault systems, and this probably facilitates the uprise of magma right in this place. It is evident that Etna lies in a very complex geodynamic environment hardly comparable to any other region on Earth. There is some evidence that Etna is but the most recent manifestation of volcanism fed from a very long-lived mantle source, having caused numerous earlier phases of mafic volcanism in the Monti Iblei, SE Sicily, from the late Triassic to the early Pleistocene.

The geological history of Mount Etna.

Mount Etna is a large basaltic composite volcano lying near the eastern coast of Sicily, in a complex geodynamic environment characterized by the collision of the African and Eurasian continental lithospheric plates. This setting contains numerous faults, including the distensive Malta-Iblei escarpment, an important structural boundary between the continental lithosphere of Sicily and the oceanic lithosphere of the Ionian sea floor. Volcanism in the area has been continuing episodically for more than 230 million years, first in the Monti Iblei, in the southeast portion of Sicily, on the foreland of the African plate promontory, and, during the past half million years, in the Etnan area.

The geological history of Etna is subdivided into four main periods (Branca et al., 2004).

a. Basal Tholeiites

The start of eruptive activity has been dated at about 500,000 years, during the mid-Pleistocene. At that time the current Etna area was occupied by a broad bay corresponding to the sedimentation base of the foredeep, and the first eruptions took place under the sea. The products of this phase of activity occur in outcrops in the area of Acicastello, Ficarazzi, and Acitrezza on the Ionian coast to the north of Catania, forming intercalations in foredeep sediments represented by grayish-blue clays of the lower to mid Pleistocene. The most famous of these outcrops is the castle rock of Acicastello, which is composed of pillow lavas and associated hyaloclastite (pillow breccias). These originally submarine products have been subjected to isostatic uplift.

b. The Timpe phase

From no less than 220,000 years ago until about 110,000 years ago, volcanic activity concentrated along the Ionian coast along a fault system known as the "Timpe" (the steps), which represents the northern continuation of the Malta-Iblei escarpment (Azzaro, 1999). The Timpe faults are marked by conspicuous morphological scarps, and terminate to the NNW near Moscarello and Sant'Alfio. During this phase, numerous fissure eruptions occurred in this relatively restricted elongate belt along the Ionian coast, and led to the growth of a NNW-SSE elongated shield volcano about 15 km long. The internal structure of this shield volcano is today exposed in the Timpe fault scarps between Acireale and Moscarello. During this eruptive period, sporadic volcanism also occurred along the valley of the Simeto river, constructing, amongst others, the large

scoria cone that constitutes the hill of Paternò and a number of thin, strongly eroded, lava flows like those cropping out in the northern periphery of Catania at Leugatia-Fasano.

c. Valle del Bove eruptive centers

About 110,000 years ago, the focus of volcanism shifted from the Ionian coast into the area now occupied by the Valle del Bove. In this period, the character of Etna's activity underwent a profound change, from sporadic fissure eruptions as during the first two phases, to a more centralized activity of both effusive and explosive character. This activity led to the construction of the first composite volcanic edifices in the Etna region, the Rocche and Tarderìa volcanoes. The products of these eruptive centers crop out along the base of the southern flank of the Valle del Bove at Tarderìa and Monte Cicirello. Subsequently, the activity concentrated in the southeastern sector of the Valle del Bove, at Piano del Trifoglietto, where the main eruptive center of this phase was built up, Trifoglietto volcano, which reached a maximum elevation of about 2400 m. Three minor eruptive centers formed subsequently on the flanks of Trifoglietto, which are named Giannicola, Salifizio and Cuvigghiuni; their activity continued until about 60,000 years ago. This phase marks the formation of a stratovolcano structure in the Etna edifice and the superposition of different eruptive centers.

d. Stratovolcano phase

About 60,000 years ago, a further shift in the focus of eruptive activity toward northwest marks the end of the Valle del Bove centers, and the start of the building of the largest eruptive center of Etna, now named Ellittico (the elliptical), which constitutes the main structure of the volcano. The Ellittico volcano produced intense effusive and explosive activity, constructing a large edifice, whose summit may have reached a height of 3600-3800 m. Numerous flank eruptions generated lava flows that reached the Simeto river valley to the west of Etna. About 25,000 years ago, the Alcantara river was deviated from its former valley closer to Etna (in correspondence with the towns of Linguaglossa and Piedimonte Etneo) into the present-day Alcantara valley (Branca, 2003). Much of the Ellittico lavas and pyroclastics are present in outcrops in the northern wall of the Valle del Bove. The Ellittico stage ended about 15,000 years ago with a series of powerful explosive (Plinian) eruptions (Coltelli et al., 2000), which destroyed the summit of the volcano leaving a caldera about 4 km in diameter. Intense eruptive activity continued during the past 15,000 years, largely filling the Ellittico caldera, and building up a new summit cone. This current summit edifice is called Mongibello. About 9000 years ago, a portion of the upper east flank of Etna underwent gravitational collapse, generating a catastrophic landslide (the Milo debris avalanche), and forming the huge collapse depression of the Valle del Bove, which still today bites deeply into the eastern sector of the volcano (Calvari et al., 2004). Following the Valle del Bove sector collapse, remobilization of the debris avalanche deposit by alluvial processes led to the generation of a detritic-alluvial deposit, known as Chiancone, which crops out between Pozzillo and Riposto along the Ionian coast. This huge collapse of the eastern flank of the Mongibello edifice has exposed a large portion of the internal structure of both the Valle del Bove eruptive centers and of the Ellittico volcano, which crop out in the walls of the depression. The eruptive activity of the Mongibello is strongly controlled by structures of weakness in the volcanic edifice, where most intrusions occur along a number of main trends. These are characterized by three main rift zones, the NE, S and W rift zones. Although much of

the activity of the Mongibello volcano is effusive, numerous strongly explosive events are known as well, mostly from the summit craters. The most powerful eruption of this eruptive phase occurred in historical time, in 122 B.C. (Coltelli et al., 1998). This eruption, which occurred from the summit of the volcano, produced a large volume of pyroclastics (ash and lapilli), which fell in a sector on the southeast flank of the volcano, causing heavy damage in the city of Catania.

### **Vesuvio test site**

Vesuvio (Vesuvius) is probably the most famous volcano on Earth, and certainly one of the most, if not the most dangerous. It is also notable for having produced the first eruption of which an eyewitness account is preserved, in AD 79. Geologically, Vesuvio is particular for its unusual versatility, its activity ranging from Hawaiian-style emission of very liquid lava, fountaining and lava lakes, over Strombolian and Vulcanian activity to violently explosive, Plinian events that produce pyroclastic flows and surges. These different eruptive styles are due to changes in the magma compositions but also to magma-water interaction (phreatomagmatic activity). Certainly the most notable aspect of Vesuvio's eminence among Earth's volcanoes is the dense population surrounding it and climbing higher and higher up its slopes. More than half a million people live in a near-continuous belt of towns and villages around the volcano, in the zone immediately threatened by future eruptions. The situation is still more peculiar as Vesuvio is not the only volcano looming above that area and its people - there is, on the other side of the city of Napoli (Naples), the caldera of Campi Flegrei, renowned for some cataclysmic ash-flow forming eruptions in the all-too-recent geologic past and signs of unrest during the past three decades. There is also the historically active volcanic complex of Ischia, not threatening to Vesuvio inhabitants but to those on Ischia island itself. Pyroclastic deposits laid down by past eruptions of Vesuvio continue to be mobilized during heavy rainfalls and can develop into catastrophic debris flows such as those of May 1998, which killed more than 150 people in the Sarno area. To complete this ensemble of geologic hazards, the area forms the nucleus of a much vaster zone that is seismically vulnerable; its most recent disastrous earthquake, on 23 November 1980, killed more than 3,000 people.

Three types of eruption are generally distinguished in the modern literature:

- a. Plinian (AD 79, Pompeii type) events with widespread airfall and major pyroclastic surges and flows;
- b. sub-Plinian to Plinian, more moderately sized eruptions (AD 472, 1631) with heavy tephra falls around the volcano and pyroclastic flows and surges;
- c. small to medium-sized, Strombolian to Vulcanian eruptions (numerous events during the 1631-1944 cycle, such as 1906 and 1944) with local heavy tephra falls and major lava flows and small pyroclastic avalanches restricted to the active cone itself.

To these three types there should be added a fourth one, though it is of the smallest dimensions of all eruption types observed at Vesuvio. It is the persistent Strombolian to Hawaiian style eruption that characterizes almost all of an eruptive sub-cycle (see below), such as was the case during the period 1913-1944. Activity of this kind is mainly restricted to the central crater where one or more intracrater cones form, and to the flanks of the cone. Lava flows from the summit crater or from subterminal vents may extend beyond the cone's base. A somewhat particular kind of persistent activity is the slow effusion of large volumes of lava from subterminal fractures to form thick piles of lava with little lateral extension, such as the lava cupola of Colle Umberto, formed in 1895-1899.

### Campi Flegrei test site

The name "Campi Flegrei" itself - "burning fields", derived from Latin and Greek words - indicates that the volcanic nature of the area has been well known since antiquity. Campi Flegrei is a volcano that you will not easily recognize at first sight when looking at it from the ground. It is a caldera, a vast volcanic collapse depression, formed during possibly more than one cataclysmic explosive eruptions, which blanketed extensive areas in the Campania region with thick deposits, mainly laid down by ground-hugging currents of gas and fragmented volcanic rocks known as pyroclastic flows. The caldera has a relatively flat floor dotted with a number of low younger volcanic features, which are mostly broad cones (tuff cones), explosion craters, and other minor features. None of these evokes the classical image of a volcano, although each one of them bears testimony to violent volcanic events in the not-too-distant past. Campi Flegrei may not look very much like a classical volcano, but it is among the most dangerous volcanoes on Earth. The highest point is barely 458 m above sea level (a portion of the caldera rim), and its largest cone, Monte Gauro, rises to a height of 331 m. Yet, while Vesuvius enjoys a status of being maybe the most famous volcano worldwide, and very much everybody knows it is close to the city of Naples, much less people know there is another volcano on the other (western) side of the megacity, and that actually a significant portion of Naples stands within the caldera of Campi Flegrei, besides the town of Pozzuoli and numerous smaller population centers. The caldera has a diameter of approximately 14 x 16 km, and shows two nested rims that are poorly defined on most sides of the volcanic complex, but instead are conspicuous on its eastern margin, where they intersect the urban area of Naples. The origin of the caldera is still subject to debate - it certainly is related to a voluminous explosive eruption about 15 ka (thousands of years) ago, the so-called Neapolitan Yellow Tuff (NYT) eruption, whereas scientists disagree whether it has also been the site of the much more voluminous "Campanian Ignimbrite" eruption about 40 ka ago. Approximately 70 smaller eruptions have occurred since the 12 ka Campanian Ignimbrite eruption, including a few dozen only during the past 4000 years. The latest eruptions, in historical time, occurred in 1198 (possibly a minor steam-blast explosion at the Solfatara) and 1538, when the small cone of Monte Nuovo (the "new mountain") was built up. Although in the past 3800 years volcanism has been at a low level - the only known events being the 1198 and 1538 eruptions - the Campi Flegrei system remains highly dynamic and restless. Long-term vertical movement of the caldera floor, that is, uplift alternating with subsidence, has been observed since antiquity, and sometimes been punctuated by episodes of accelerated uplift. Rapid uplift preceded the 1538 Monte Nuovo eruption, and occurred again during two well-documented episodes in 1969-1972 and 1982-1984, without culminating in renewed volcanism - thus far. These latest episodes of unrest, which were accompanied by increased seismic activity, have triggered intense studies of the Campi Flegrei volcanism and related hazards. At present (2011), the Campi Flegrei volcano shows relatively low levels of unrest, although minor episodes of ground uplift and slightly elevated seismic activity have occurred repeatedly since the end of the most recent major crisis in the mid-1980s. However, in a recent publication Isaia et al. (2004) note that about 4000 years ago a series of 15 eruptions occurred during an interval of 150 years, sometimes simultaneously in the western and eastern portions of the caldera. They furthermore found evidence for several tens of meters of ground uplift in the caldera prior to this intense eruptive period and speculate that the renewed unrest observed since 1969 might be a precursor of similar activity in the future.

## 5. ASI-SRV pre-operative processors

The efforts to satisfy the requests for operative support expressed by the Italian DPC by means of spaceborne and airborne image data is at the base of all technical design and development of ASI-SRV by producing a system concept based on flexible modules which are needed to take into account the new coming space sensors, new processing algorithms and Web-GIS interfaces considering the national and international scenario in the space technologies. Starting from the modular approach the system should be able to produce all the requested information relative to the volcanic activity phases corresponding to the end user operative protocols which are:

1. Early Warning: it identify and measure variations in the state of the volcanic area before the eruption
2. Crisis: it support organizations involved in the management of emergency situations in order to activate the planned procedures in the case of a possible emergency in the volcanic areas
3. Post Crisis: it analysis of effects produced by the eruption

The Project has included a long and continuous demonstration phase during which time series for all the EO data, both optical and radar have been systematically used to generate upgraded added values product as soon as a new acquisition is available. Considering that an important step of the project development regarded the technical and scientific feasibility of the selected products a technical feasibility has been executed highlighting the dependencies from the data availability (in terms of spectral channel, satellite revisit time, accuracy algorithms and models used in the processing).

The algorithms selected for the EO processing modules have been analyzed during the last decade and have the following characteristics:

- Robust with a well proved scientific background
- High Adaptability to new space sensor
- Portability into an integrates system
- The algorithms were developed in house (INGV, CNR-IREA, University of Modena and Reggio Emilia) which ensure the possibility to upgrade the procedures and adapt them to ASI-SRV system
- Products partially tested in other Projects or INGV surveillance Procedures
- Suitability of the generated products for the selected test sites

In general two classes of products are generated respectively concerning radar and optical remote sensed data. A first important class of products regard the characteristics derived by active sensors such as the deformation maps retrieved by SAR interferometry which is based on consolidated techniques [Lanari et al. 2004], and the accuracy has been analyzed in the past years. Moreover the selected test sites have well developed GPS network that ensure a suitable validation for the SAR maps produced by the system. Nevertheless the usability of the deformation maps in the Crisis Phase (Sin-eruptive) is restricted by the low revisit time of the current systems. Within the ASI-SRV project since the availability of new mission (eg. COSMO-SKYMED) the improvement of the revisit time as well as the ground resolution of SAR systems in a prototype procedures have been developed and tested. A second class of product regards the analysis products derived by passive sensors. The available algorithms allow to extract information, such as the surface thermal characteristics, during both the Early Warning phase and during the Crisis phase. In the Early Warning phase the thermal analysis is directed to the identification of temperature variation on

volcanic structure which may indicate a change in the volcanic activity state [Realmuto, 1990]. The feasibility of this product depends from the availability of bands the TIR region and from the accuracy of the atmospheric corrections applied to the images. A major operative limitation for this product is the very low spatial resolution in the TIR channels for space sensors with an high revisit time (>1km pixel). At the moment the only sensor that present good technical characteristics for the Early Warning is the ASTER sensor (90 m pixel) on NASA satellite TERRA, the lack of future missions with high spatial resolution in the TIR region may prevent an effective support in the early warning phase of volcanic activity by space sensors. The product regarding the Crisis stage is mainly finalized to the estimation of the effusion rate for active lava flows, the algorithms for this product are well consolidated and could be applied to the low spatial resolution space sensors (eg. AVHRR, MODIS, MSG) [Lombardo et al. 2004]. Moreover the analysis of the emitted gas species from degassing plume is usually performed through ground networks of instruments based on the spectral behaviour of the gas species, although many volcanoes in the world do not have such permanent networks. The ASI-SRV system will produce information on the concentration and flux of sulphur dioxide (SO<sub>2</sub>) [Realmuto et al., 1994] water vapour and volcanic aerosol optical thickness [Spinetti et al., 2003] by means of ASTER, MODIS and HYPERION data on Etna test site. The analysis of ash clouds will be made by means of already consolidated procedures [Searcy et al., 1998, Corradini et al., 2006, Constantine et al., 1999] which uses low spatial resolution sensors with an high revisit time (eg. AVHRR, MODIS). For the Post Crisis phase the required products will be obtained through classification algorithms and spectral analysis.

## 5.1 ASI-SRV: Early warning phase products

### 5.1.1 Ground deformation analysis using SAR time series

The algorithm selected for ground deformation analysis via the use of SAR data is the Small Baseline Subset (SBAS) approach described in details in Berardino et al., 2002 and Lanari et al., 2004. This algorithm has the unique capability to work at both low and full spatial resolution scales. While full resolution scale has an impact in monitoring single structures (which are generally not visible at the larger spatial scale), it has been demonstrated in the literature that the low spatial resolution scale results (100 m pixel spacing) are well suited to characterize and monitor volcanic phenomena (Figure 5). This has the big advantage of reducing the amount of data to be handled, thus making the whole processing chain more efficient with respect to the full resolution one. The achievable accuracy has also been extensively tested by comparison with classical geodetic measurements (levelling, continuous GPS, alignment arrays, etc.). For a typical data set of 40-50 ESA SAR images in a time span of 10 years the calculated accuracies are generally lower than: 2 mm/year on the mean velocity and 10 mm on the ground deformation time series; more details can be found in Lanari et al., 2007 and Casu et al., 2006.

### 5.1.2 Surface temperature, emissivity and thermal flux

The surface temperature and emissivity processing module gives as output result the surface temperature map and the spectral emissivity image. The spectral radiance emitted by a body having a kinetic temperature  $T_s$  can be expressed as a function of the spectral emissivity  $\varepsilon$  of its surface and of the Planck function  $B$ :

$$L(\lambda, T_s) = \varepsilon(\lambda) \cdot B(\lambda, T_s) \quad (1)$$

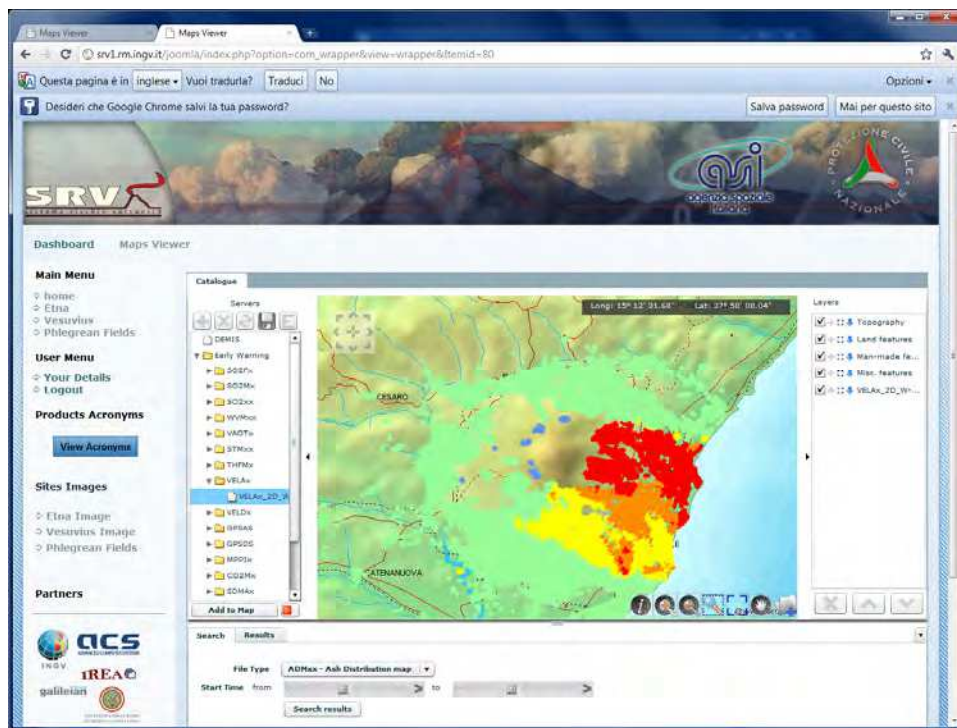


Fig. 5. Example of ground deformation product that is provided for all test sites and for both orbit (ascending and descending)

If the radiance  $L$  is measured at  $N$  wavelengths  $\lambda$ , the relation is expressed by a system of  $N$  equations with  $N+1$  unknowns, i.e. the  $N$  values of spectral emissivity and the temperature. This makes difficult the estimation of surface temperature and emissivity from remote sensing data because the equation system is not closed. In the literature, different “non-exact” solutions are given to this problem, called Temperature and Emissivity Separation (TES). Details of the different algorithms that have been proposed so far are discussed in [Gillespie, 1998, ; Li et al., 1999]. In this project we use the TES algorithm [Gillespie, 1998] and where not possible the well established method of the Emissivity Spectrum Normalization (ESN) [Gillespie, 1985; Realmuto, 1990]. These methods are robust and have demonstrated a good capability to maintain the spectrum shape, that is the most important feature in applications of spectral analysis and mapping.

During the monitoring and early warning phases the thermal flux can be estimated from ASTER images. Input to the module are the surface temperature and emissivity retrieved by the TES module and the output is the estimated thermal flux map.

The surface temperature and emissivity retrieved by means of the TES module allow the estimate of the surface emitted thermal flux and the production of the related maps. The radiant flux  $Q_{rad}$  emitted by a surface element of area  $A$  at given temperature and emissivity is

$$Q_{rad} = \epsilon \sigma A T^4 \quad (2)$$

where  $\sigma$  is the Stefan-Boltzmann constant. Inputs to the module that estimates the thermal flux are thus the TES module surface temperature and emissivity, while the output is the Qrad image. (Figure 6)

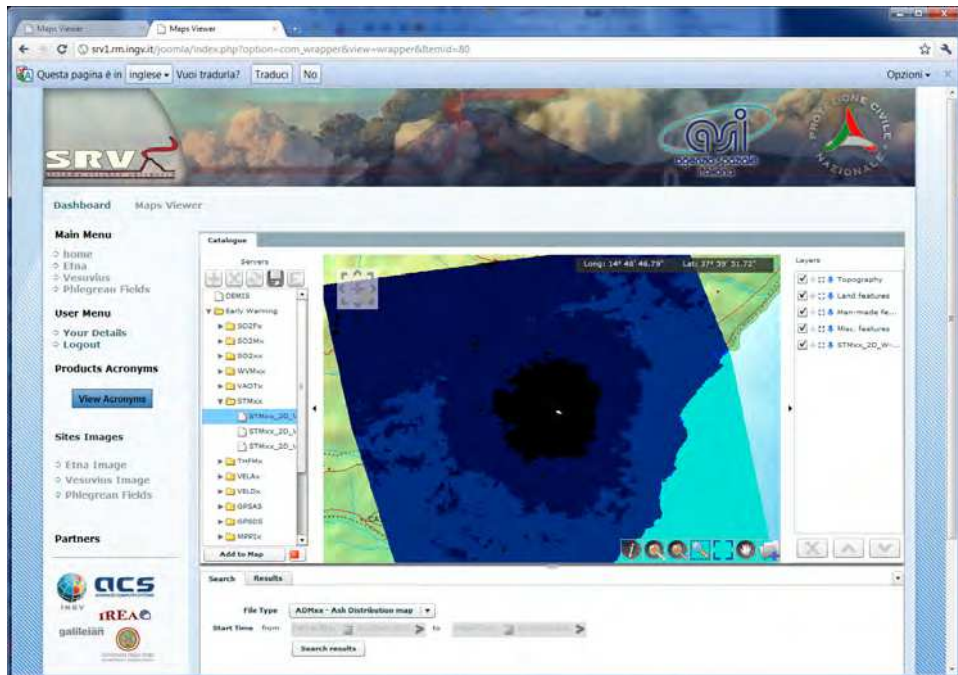


Fig. 6. Example of surface temperature product. It can be obtained by ASTER (nighttime in figure) by MODIS and AVHRR.

### 5.1.3 VAOT Volcanic aerosol optical thickness estimation

The VAOT has been developed at INGV [Spinetti et al., 2003, Spinetti et al., 2004, Spinetti and Buongiorno 2007], and represents the first algorithm that has been developed following the theoretical basis of atmospheric aerosol estimated from space, published by [Kaufman 1997]. Purpose of this algorithm is the estimation of the volcanic aerosol optical thickness (AOT) during the prevention and early warning phase therefore VAOT technique has been used in ASI-SRV to estimate AOT at medium-high resolution in early warning phase. The algorithm to estimate the AOT parameter is based on the inversion of the radiative transfer equation using the 6S [Vermote 1997] radiative transfer code. (Figure 7)

### 5.1.4 Water vapour estimation

The used algorithm to estimate the volcanic water vapour in a volcanic plume has been developed at INGV [Spinetti et al., 2003, Spinetti et al., 2004]. This has been developed on the well consolidated theoretical basis of atmospheric water vapour estimation published by [Carrere and Conel, 1993]. Purpose of this algorithm, which is based on the fitting of the simulated radiance to the effectively one measured, is the estimation of the volcanic plume



water vapour.. The band used is the 1130 nm as the 940 nm band shows a problem in overlapping signals. (Fig. 1)

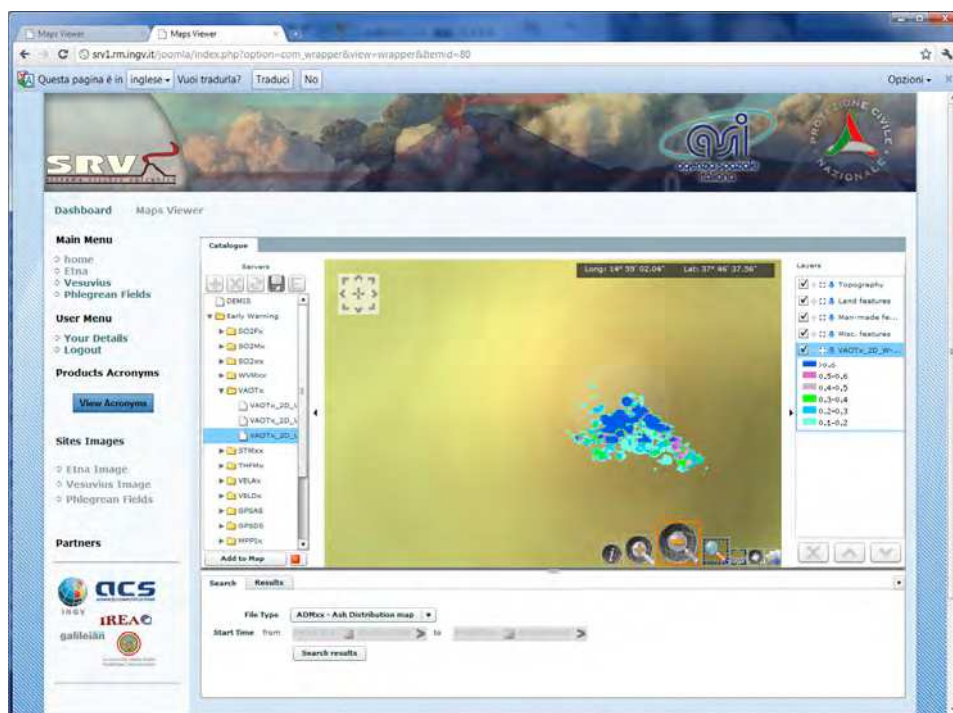


Fig. 7. Example of aerosol optical depth provided by means of official gateway. During early warning phase this product is generated by high spatial resolution sensor

## 5.2 ASI-SRV sin eruption phase

### 5.2.1 SAR deformation map production using interferogram couple module

For measuring ground deformations during sin-eruptive phase, the ASI-SRV will use the Two-Pass interferometric process (Zebker & Goldstein, 1986; Massonet & Feigl 1998). This choice allows measuring ground deformations by using a single SAR image pairs, provided by any SAR sensor. This approach does not require minimum critical dimension of the number of images in the database and, furthermore, allows using SAR data provided from different sensors (e.g. ENVISAT, RADARSAT, etc.). The only constraint in applying this method is to have a good correlation between the image pairs. (Fig. 2)

### 5.2.2 Thermal flux and effusion rate computation modules

For the estimation of the Effusion Rate the dual band algorithm has been implemented. The dual-band technique allows a realistic estimate of the energy flux radiated from active lava flows and fumaroles [Pieri et al., 1990, Wright et al., 2000]. The thermal model for active lava flows considers the thermal flux as a function of the fractional area of two thermally distinct radiant surfaces. Within this model, the larger surface area corresponds to the cooler crust of

the flow and the other, a much smaller area, to fractures in the crust. These cracks are at much higher temperatures than the crust and are closer to the temperature of the molten or plastic flow interior. Interior temperatures for active lava flows are typically about a factor 2-4 higher than that of the crust [Calvari et al., 1994, Flynn et al., 1993]. The dual-band method requires two distinct SWIR bands ( $\alpha$  and  $\beta$ ) to formulate a system of two equations from the simultaneous solution of the Planck equation in each band. Solution of these simultaneous equations allows calculation of the 'sub-pixel' coverage and temperature of the crusted and hot components. The dual-band general formula is written as:

$$\text{Rad}\alpha = f_h (\text{Rh}\alpha) + (1 - f_h) \text{Rc}\alpha \quad (3)$$

$$\text{Rad}\beta = f_h (\text{Rh}\beta) + (1 - f_h) \text{Rc}\beta$$

where  $\text{Rad}\alpha$  and  $\text{Rad}\beta$  are respectively the total radiance detected by the sensor in band  $\alpha$  and  $\beta$ ,  $\text{Rh}\alpha$  is the radiance of the hot crack component in band  $\alpha$  ( $\alpha = \alpha$  or  $\beta$  in our case),  $\text{Rc}\alpha$  is the radiance of the cooler crust component in band  $\alpha$  and  $f_h$  is the fractional area of the pixel with hottest temperature  $T_h$ . Following [Oppenheimer, 1991, Harris et al., 1998, Flynn et al., 2000] we can solve the system by assuming a value for  $T_h$ , to obtain values for the two unknowns.

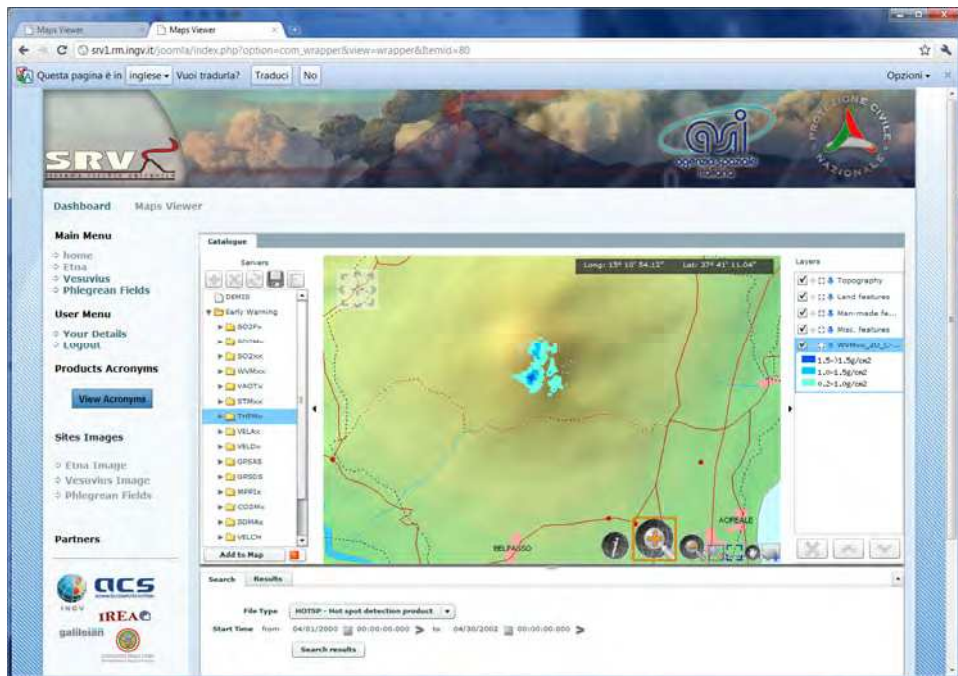


Fig. 1. Example of water vapour content provided by means of official gateway

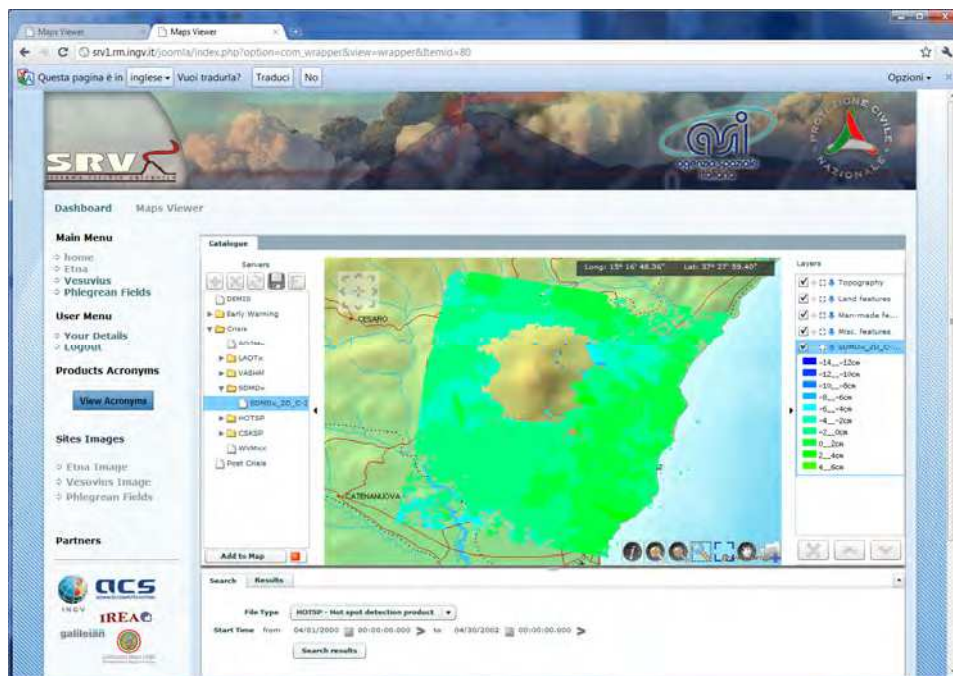


Fig. 2. Example of sin eruptive deformation map provided by means of official gateway

The main information layer is the temperature of the thermal anomaly and its spatial location. The thermal flux map is derived from the temperature maps retrieved using the dual-band technique and it is expressed in watt. Thermal flux roughly represents the energy emitted by the hot-spot when the image has been acquired. Effusion rate appears to control the basic flow dynamics and the manner of emplacements of active flows. Therefore measurements of the effusion rate are of great interest. Reliable estimations of  $E_r$  imply the knowledge of rheological and geological parameters such as the lava density, the specific heat capacity, the temperature drop throughout the moving portion of the flow and the mass fraction of crystal grown through the cooling process. These parameters are typical of each different volcano and must be separately estimated or derived from literature. (Fig. 3)

### 5.2.3 Sulphur dioxide retrieval modules

Three different procedure are able to estimate the sulphur dioxide from a volcanic source: LUT [Realmutto et al., 1997], FUN [Teggi et al., 1999] SW [Pugnaghi et al., 1999, Pugnaghi et al., 2002] which doesn't require the DEM. All these three mentioned procedures have been implemented in the ASI-SRV system to estimate the sulphur dioxide emitted from Mt. Etna. The routinely measurements of the  $SO_2$  volcanic flux is important because its variation from the standard baseline can be used as precursor of possible start or end of an eruption [Caltabiano et al., 1994]. In the thermal infrared (TIR) portion of the electromagnetic spectrum a common and good assumption, in absence of clouds, is that scattering is negligible. If there is no scattering, the spectral radiance at the sensor, in the 8-14  $\mu m$  atmospheric window, depends on the radiance from the surface (which mainly depends on

temperature and emissivity) and on the effect of the atmospheric path between the target and sensor.

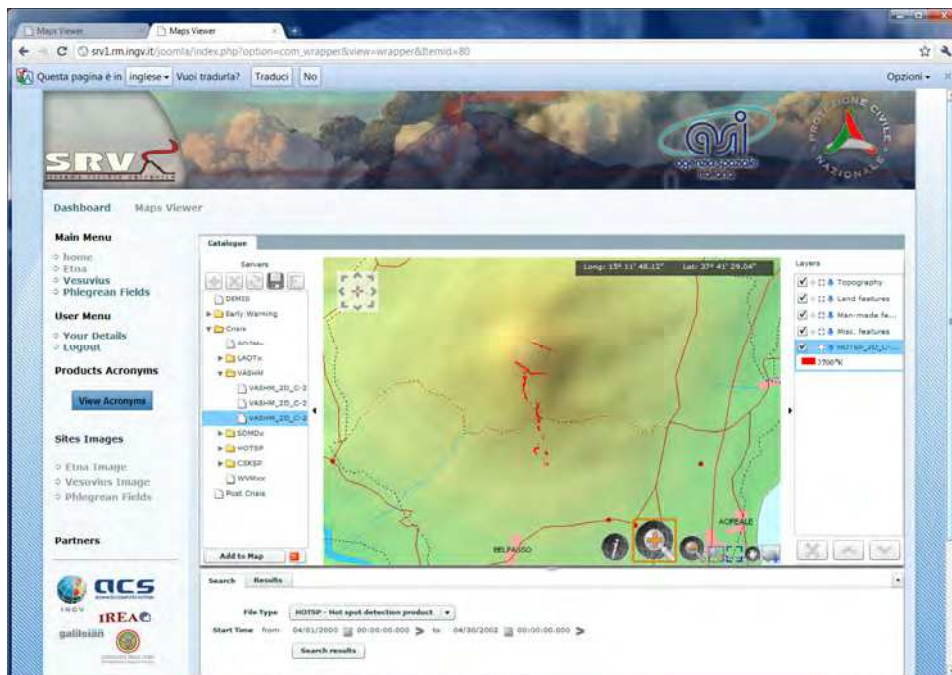


Fig. 3. Example of sin eruptive surface thermal map map provided by means of official gateway

To compute the sulphur dioxide flux ( $F$ ) emitted from the volcano vents, the map of the columnar content of  $\text{SO}_2$  ( $c_s$ ), computed from the remotely sensed image, and the wind speed ( $v$ ) measured at the plume altitude are required. The plume axis and the transect length (or plume width) have to be chosen by the user on the sulphur dioxide map, which is the result of the previous algorithm (Fig. 4).

$$F = v \cdot \int c_s \cdot ds \quad (4)$$

#### 5.2.4 Low aerosol optical thickness (LAOT) estimation

In order to estimate the Volcanic Aerosol Optical Thickness in a volcanic plume during crisis, an algorithm called LAOT based on low spatial resolution image has been implemented in the ASI-SRV system. This algorithm based on the same approach described in VAOT has been developed at the Univeristy of Modena [Remitti et al., 2006]. This algorithm is based on the work of [Kaufman 1993, Kaufman et al., 1997 and Remer et al., 2005] (Fig. 5).



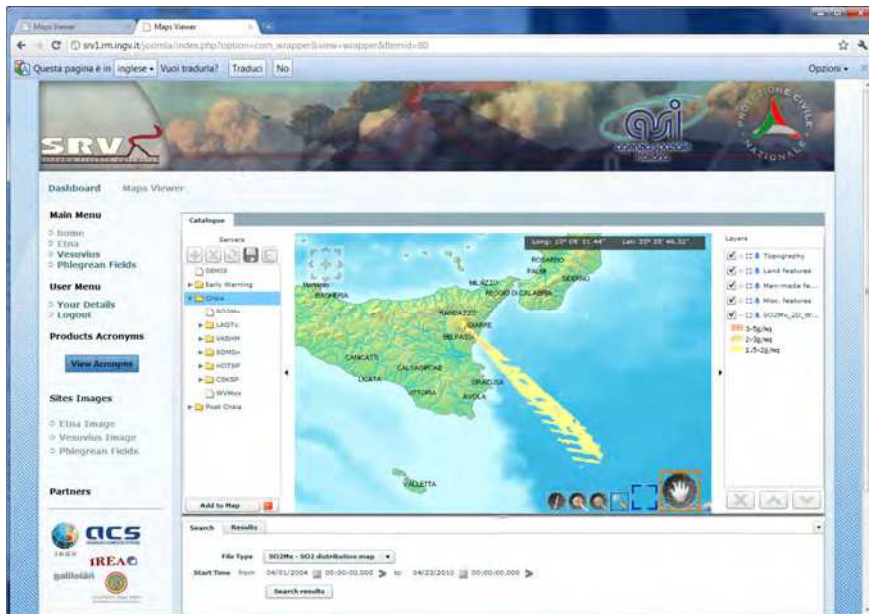


Fig. 4. Example of SO<sub>2</sub> map product generated and delivered by means of dedicated gateway

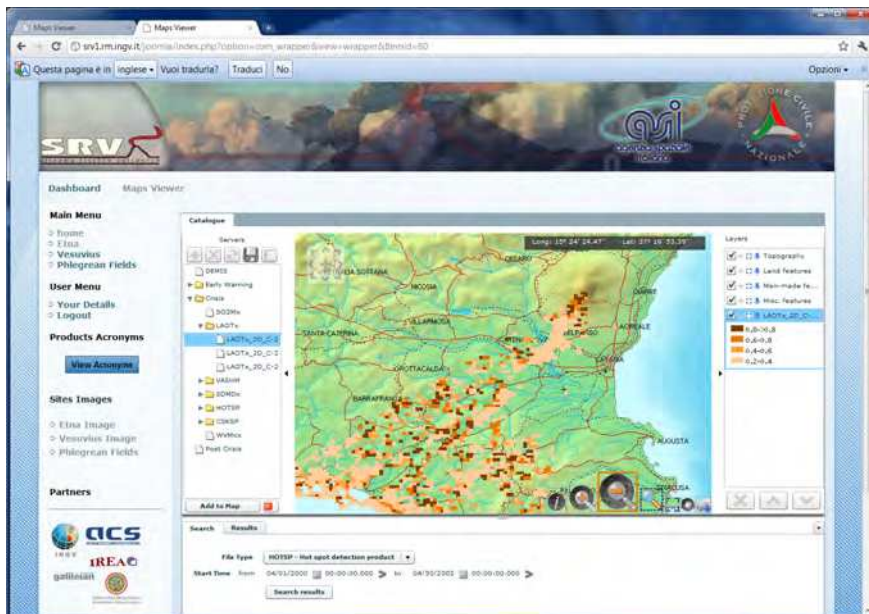


Fig. 5. Example of aerosol optical depth provided by means of official gateway. During crisis phase this product is generated by low spatial resolution sensor

### 5.2.5 Volcanic ash loading map (VAMP)

Purpose of this algorithm is the volcanic ash detection and loading retrieval from MODIS spaceborne measurements in Thermal InfraRed (TIR) spectral range. The algorithm is based on Brightness Temperature Difference (BTD) procedure [Prata and Barton, 1989] applied on MODIS channels 31 and 32. The ash detection is realized inverting the Planck function, computing the brightness temperatures for the cited channels and making the difference. The ash detection is obtained showing the BTD map [°C] and identifying the negative values. The ash loading map retrieval [tons] is performed using the effective radius (reff) and aerosol optical thickness (AOT) retrieval obtained by a double linear interpolation from the AOT-reff curves computed using the simulated Top Of Atmosphere (TOA) radiances [Wen and Rose, 1994]. The simulated radiances will be estimated from MODTRAN Radiative Transfer Model (RTM) [Berk et al., 1989], using as input the atmospheric profiles (pressure, temperature, humidity), surface characteristics (temperature, emissivity) and ash optical properties (extinction coefficient, absorption coefficient, asymmetry parameter). The total plume ash loading is computed as sum of the retrieved ash loading of each pixel. (Fig. 6).

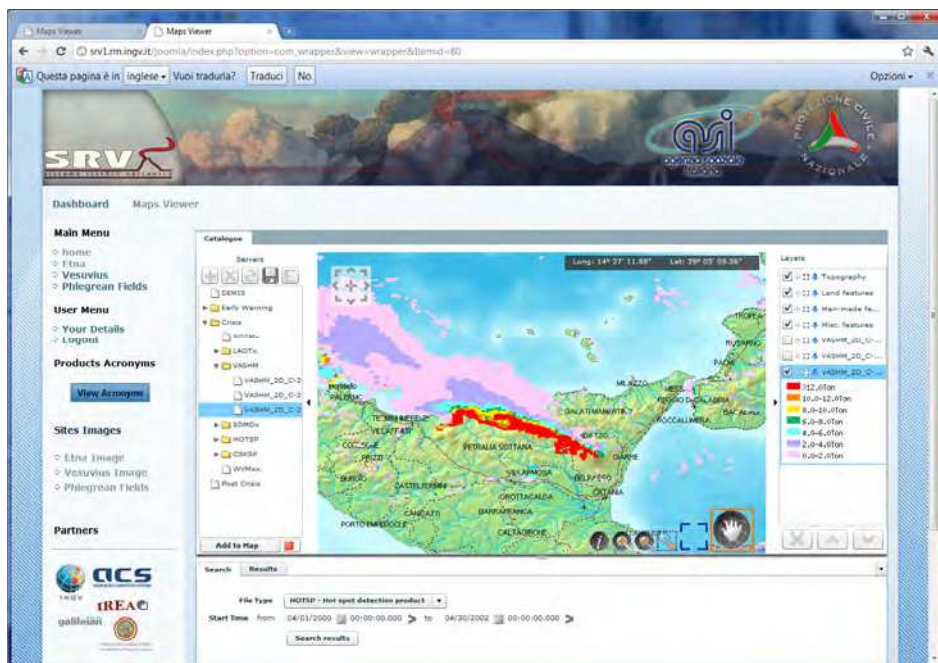


Fig. 6. Example of ASH map product generated and delivered by means of dedicated gateway

### 5.3 ASI-SRV POST ERUPTION PHASE

Active volcanoes that erupt frequently constantly change in shape and volume. Mount Etna produces major lava flows about once per year, and more explosive activity is nearly always accompanied by growth of pyroclastic cones, whereas inter-eruptive intervals may be marked by collapse of portions of the summit cones. These morphological changes strongly

influence the distribution of future eruptive products (namely lava flows) and need to be carefully mapped and measured for the assessment of the hazard from future eruptions. The new distribution of ash and lava flow have been evaluated by means of spectral classification using supervised and unsupervised technique. Beside this surface classification an evaluation of the thickness of eruptive products will be carried out in the field, using hand-held GPS to create a model of the new, post-eruptive surface morphology in areas affected by the eruptive activity. GPS is the instrument most suitable for obtaining a high quantity of data at a resolution comparable to that of the satellite images used for the project. This new morphology will be superimposed on the pre-eruptive morphology to reveal the approximate ( $\pm 5$  m) thickness of the new products in any site, and obtain volume estimates (Fig. 7).

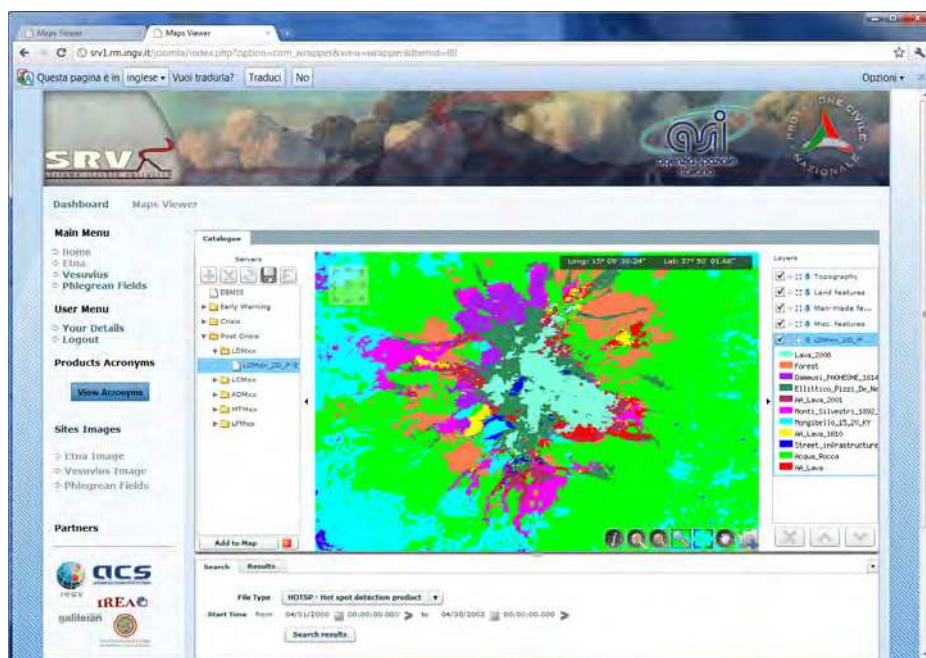


Fig. 7. Example of post eruptive lava distribution map product generated and delivered by means of dedicated gateway

### 5.3.1 Multiparametric analysis

All the above mentioned early-warning products have been used to verify the capability of dedicated statistical model to support the monitoring activities. ASI-SRV project has implemented a well-known model called Bayesian Event Tree – Eruption Forecast (BET-EF) (Marzocchi et al., 2009) which is an already developed algorithm for the eruption model, and has been adapt, as it is, to the ASI-SRV needs. The BET-EF model represents a flexible tool to provide probabilities of any specific event at which we are interested in, by merging any kind of available and relevant information, such as theoretical models, a priori beliefs, monitoring measures, and real time and past data. It is mainly based on a Bayesian



procedure and it relies on the fuzzy approach to manage monitoring data. The method deals with short- and long-term forecasting, therefore it can be useful in many practical aspects, as land use planning, and during volcanic emergencies. Besides BET-EF a multivariate analysis allows to perform multiple comparisons in order to have a first idea of which variables are largely preferentially or rather rarely distributed, also considering their geographic localization, and then a cross correlation will allow to define the weight of each product that will be used as input in the BET-EF model (Fig. 8).

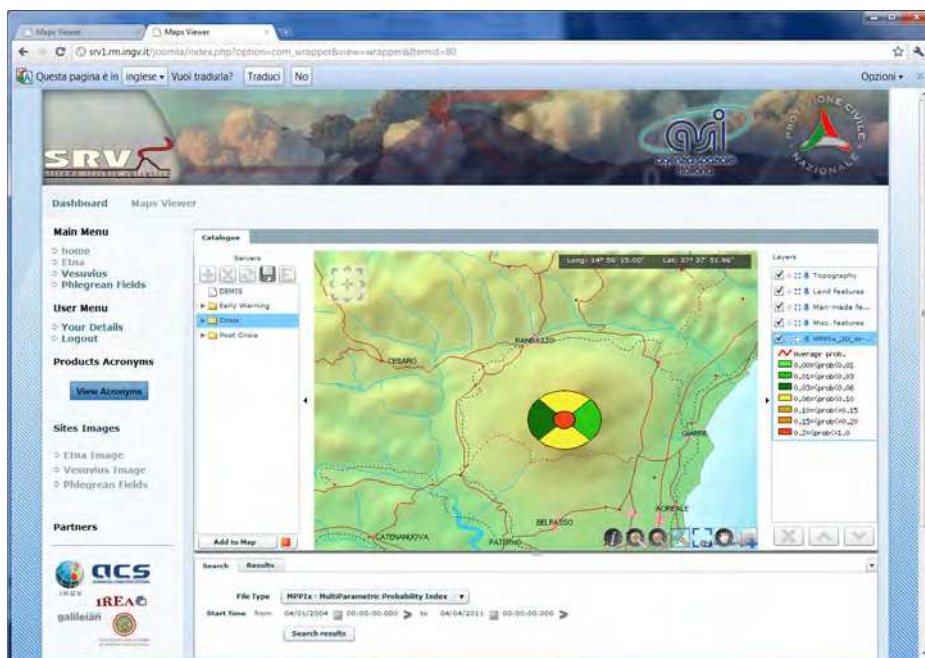


Fig. 8. Example of ASH map product generated and delivered by means of dedicated gateway

## 6. Conclusion

Technologies and services provided by ASI-SRV are developed for provide added value information in case of Volcanoes eruption, but also during the pre-event (early warning) phase and post-event enabling an improved support for risk management and assessment. In order to let remote sensed data available to the core processes as soon as they are received selected processors operating in un-supervised mode generate advanced L1 data.

The processing chains has been delocalized ensuring the fastest updating rate for the newest generated products. The processing chain for radar data has been located and operated at IREA premises and the processing results will be transferred to the main system via ftp connection as soon as they are generated. This choice is justified essentially its high complexity, the algorithm must be supervised during the whole processing phase by an expert operator who is also responsible for setting a number of important parameters that



affect the quality of the final result: Expert personnel operate the module throughout the project lifetime.

The processing chain dedicated to the develop of product by optical remote sensed data has been located and operated at INGV premises and the processing results are transferred to the project gateway by means of dedicated procedure for validation and dissemination as soon as they are generated.

The availability of a set of instrument dedicated to the harmonization and pre-processing of EO data represents an important tool for a complex system as ASI-SRV is. A well structured production chain, that manage the ingestion, pre processing, processing and publication of EO derived product in a semi-automatic process, allow to compare a wide volume of data using the same standard. All the validated ASI-SRV products produced by processing modules and data processor software are stored in the ASI-SRV main database, in order to be published by Web-GIS and then made available to the end-user.

SRV project has finished the development of architectural design of modules and interfaces and it is now ready to operate according the User's request.

## 7. Acknowledgment

This study was supported by Agenzia Spaziale Italiana Progetto Sistema Rischio Vulcanico project (ASI-SRV ref ASI I/091/06/0). The active contribute of the Italian DPC has been very important in order to meet the requirement requested especially regarding the delivery time of the products in the Crisis Phase.

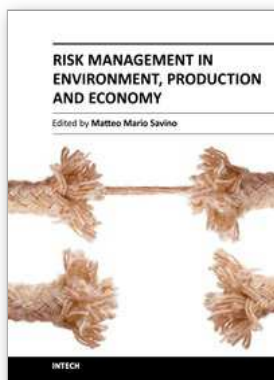
## 8. References

- Azzaro R. (1999) Earthquake surface faulting at Mount Etna volcano (Sicily) and implications for active tectonics. *J. Geodyn.*, 28, 193-213.
- Berardino, P., Fornaro, G., Lanari, R., and Sansosti, E. (2002), A new Algorithm for Surface Deformation Monitoring based on Small Baseline Differential SAR Interferograms, *IEEE Transactions on Geoscience and Remote Sensing*, 40, 11, 2375-2383.
- Berk A., Bernstein L.S. e Robertson D.C..( 1989) MODTRAN: a moderate resolution model for Lowtran7, GL-TR-89-0122, AFG Lab., Hanscom Air Force Base, MA 01731-5000, USA.
- Branca S. (2003) Geological and geomorphologic evolution of the Etna volcano NE flank and relationships between lava flow invasions and erosional processes in the Alcantara Valley (Italy). *Geomorphology*, 53, 247-261.
- Branca S., Coltelli M., De Beni E., Wijbrans J. (2008) Geological evolution of Mount Etna volcano (Italy) from earliest products until the first central volcanism (between 500 and 100 ka ago) inferred from geochronological and stratigraphic data. *Intern. J. Earth Sci.*, 97:135-152
- Branca S., Coltelli M., Groppelli G. (2004) Geological evolution of Etna volcano. In: "Etna Volcano Laboratory" Bonaccorso, Calvari, Coltelli, Del Negro, Falsaperla (Eds), AGU (Geophysical monograph) 143, pp 49-63.
- Caltabiano T., Romano R., Budetta G., (1994). SO<sub>2</sub> flux measurements at Mount Etna (Sicily). *Jour. Geoph. Res.*, 99, D6, 12.809-12.819

- Calvari S., Neri M., Pompilio M., Scribano V., (1994). Etna: Eruptive activity. In: "Data related to eruptive activity, unrest phenomena and other observations on the Italian active volcanoes - 1992", L. Villari (Ed.), *Acta Vulcanol.*, 6, 1-3
- Calvari, S., Tanner, L.H., Groppelli, G., Norini, G. (2004) A comprehensive model for the opening of the Valle del Bove depression and hazard evaluation for the eastern flank of Etna volcano. In: "Etna Volcano Laboratory" Bonaccorso, Calvari, Coltelli, Del Negro, Falsaperla (Eds), AGU (Geophysical monograph) 143, pp 65-75.
- Coltelli M., Del Carlo P., Vezzoli L. (2000) Stratigraphic constrains for explosive activity in the last 100 ka at Etna volcano. Italy. *Inter. J. Earth Sciences* 89: 665-677.
- Coltelli, M., Del Carlo, P., Vezzoli, L. (1998) The discovery of a Plinian basaltic eruption of Roman age at Etna volcano, Italy. *Geology*, 26, 1095-1098.
- Flynn LP, Harris AJL, Rothery DA, Oppenheimer C (2000) High-Spatial resolution thermal remote sensing of active volcanic features using Landsat and hyperspectral data. *Remote Sensing of Active Volcanism AGU Geophysical Monograph Series* 116: 161-177.
- Flynn, L., P. Mouginis-Mark, J. Gradie, and P. Lucey, (1993) Radiative Temperature Measurements at Kupaianaha Lava Lake, Kilauea Volcano, Hawaii, *J. Geophys. Res.*, 98, 6461 - 6476
- Gillespie, A., Rokugawa, S., Matsunaga, T., Cothorn, J.S., Hook, S. And Kahle, A. (1998): A temperature and emissivity separation algorithm for Advanced Spaceborne Thermal Emission and Reflection Radiometer (ASTER) images, *IEEE Trans. Geosci. Remote Sensing*, 36 (4), 1113-1126
- Gillespie, A.R. (1985): Lithologic mapping of silicate rocks using TIMS, in *The TIMS Data User's Workshop*, JPL Publication 86-38, Jet Propulsion Lab., Pasadena, CA, 29-44
- Harris, A.J.L., Flynn, L.P., Keszthelyi, L., Mouginis-Mark, P.J., Rowland, S.K., Resing, J.A., (1998). Calculation of lava effusion rates from Landsat TM data, *Bull. Vulcanol.* 60, 52-71.
- Isaia R., M. D'Antonio, F. Dell'Erba, M.A. Di Vito and G. Orsi, (2004) The Astroni volcano: the only example of close eruptions within the same vent area in the recent history of the Campi Flegrei caldera (Italy), *Journal of Volcanology and Geothermal Research* 133, pp. 171-192.
- Kaufman Y.J., Tanre' D., Remer L.A., Vermote E.F., Chu A., Holben B.N., (1997). Operational remote sensing of tropospheric aerosol over land from EOS moderate resolution imaging spectroradiometer. *Journal of Geophysical Research*, Vol. 102, No. D14, pp. 17,051-17,067, July 27.
- Kaufman, Y. J. (1993) "Measurements of the aerosol optical thickness and the path radiance - Implications on aerosol remote sensing and atmospheric corrections", *Journal of Geophysical Research*, 98, 2677-2692, (b)
- Kaufman, Y.J. Wald, A.E. Remer, L.A. Bo-Cai Gao Rong-Rong Li Flynn, L. (1997) The MODIS 2.1- $\mu\text{m}$  channel-correlation with visible reflectance for use in remote sensing of aerosol Geoscience and Remote Sensing, *IEEE Transactions on Publication Date: Sep Volume: 35, Issue: 5*
- Lanari, R., De Natale, G., Berardino, P., Sansosti, E., Ricciardi, G. P., Borgstrom, S., Capuano, P., Pingue, F., and Troise, C. (2002), Evidence for a peculiar style of ground deformation inferred at Vesuvius volcano, *Geophysical Research Letters*, 29

- Lanari, R., Lundgren, P., Manzo, M., and Casu, F., (2004b), Satellite radar interferometry time series analysis of surface deformation for Los Angeles, California, *Geophysical Research Letters*, 31, L23613, doi:10.1029/2004GL021294.
- Lentini F., Carbone S., Catalano S., Grasso, M. (1996) Elementi per la ricostruzione del quadro strutturale della Sicilia orientale. *Mem. Soc. Geol. It.*, 51, 179-195.
- Li, Z., Becker, F., Stoll, M. And Wan, Z. (1999): Evaluation of six methods for extracting relative emissivity spectra from thermal infrared images, *Remote Sens. of Env.*, 69, 197-214.
- Lundgren, P., Casu, F., Manzo, M., Pepe, A., Berardino, P., Sansosti, E., and Lanari, R. (2004), Gravity and magma induced spreading of Mount Etna volcano revealed by satellite radar interferometry, *Geophysical Research Letters*, 31, L04602, doi:10.1029/2003GL018736
- Manzo M., Ricciardi, G. P., Casu, F., Ventura, G., Zeni, G., Borgström, S., Berardino, P., Del Gaudio, C. and Lanari, R. (2006), Surface deformation analysis in the Ischia island (Italy) based on spaceborne radar interferometry, *Journal of Volcanology and Geothermal Research*, 151, 399–416, doi:10.1016/j.jvolgeores.2005.09.010.
- Marzocchi, W., Sandri, L., Selva J., (2009) BET\_EF: a probabilistic tool for long- and short term eruption forecasting, *Bull. Volcanol.*, doi:10.1007/s00445-007-0157-y,
- Massonet D., K. Feigl, (1998) Radar Interferometry and its application to changes in the Earth's surface, *Reviews of Geophysics*, 36, 4 / November 1998, pag. 441-500,
- Oppenheimer, C., (1991). Lava flow cooling estimated from Landsat Thematic Mapper infrared data: The Lonquimay eruption (Chile, 1989), *Journal of Geophysical Research* 96, 21865-21878.
- Pepe, A., E. Sansosti, P. Berardino and R. Lanari (2005), On the Generation of ERS/ENVISAT DinSAR Time-Series via the SBAS technique, *IEEE Geoscience and Remote Sensing Letters*, 2, 3, pp. 265-269.
- Pieri, D.C., Glaze, L.S., Abrams, M.J., (1990). Thermal radiance observation of an active lava flow during the June 1984 eruption of Mt. Etna, *Geology*, v.18, 1018-1022
- Prata A. J., I. J. Barton, (1989) "Detection and discrimination of volcanic clouds by infrared radiometry - I: theory", *Proc. of the first international symposium on Volcanic ash and aviation safety*, 305-311.
- Pugnaghi S., Gangale G., Corradini S., Buongiorno M.F. (2006), Mt. Etna sulfur dioxide flux monitoring using ASTER-TIR data and atmospheric observations, *Journal of Volcanology and Geothermal Research*, 152, 74–90.
- Pugnaghi, S., Teggi, S., Corradini, S., Buongiorno, M.F., Merucci, L., Bogliolo, M.P., (2002). Estimation of SO<sub>2</sub> abundance in the eruption plume of Mt. Etna using two MIVIS thermal infrared channels: a case study from the Sicily-1997 Campaign. *Bull Volcanol* 64, 328-337.
- Realmuto, V.J. (1990): Separating the effects of temperature and emissivity: emissivity spectrum normalization, in *Proc. 2nd TIMS Workshop*, JPL Publication, 90-55, Jet Propulsion Lab., Pasadena, CA.
- Realmuto, VJ, AJ Sutton and T Elias (1997) Multispectral thermal infrared mapping of sulfur dioxide plumes - a case study from the East Rift Zone of Kilauea volcano, Hawaii, *Jour. Geophys. Res.*, 102: 15057-15072
- Remer, L. A. Kaufman, Y. J. Tanrè, D. Mattoo, S. Chu, D. A. Martins, J. V. Li, R.-R. Ichoku, C. Levy, R. C. Kleidman, R. G. Eck, T. F. Vermote E. and Holben, B. N. (2005) "The

- MODIS Aerosol Algorithm, Products and Validation", *Journal of Atmospheric Science*, Special Section, 62, 947-973.
- Remitti M., Pugnaghi S., Teggi S., Parmiggiani F., (2006). Retrieval of tropospheric ash clouds of mt. etna from AVHRR data *Quaderni di Geofisica* n. 43.
- Spinetti C. and M.F. Buongiorno, (2007). Volcanic Aerosol Optical Characteristics of Mt. Etna Tropospheric Plume Retrieved by Means of Airborne Multispectral Images. *Journal of Atmospheric and Solar-Terrestrial Physics* Volume 69, Issue 9, pp. 981-994 doi:10.1016/j.jastp.2007.03.014.
- Spinetti C., Buongiorno M.F., Lombardo V., Merucci L. (2003) - Aerosol optical thickness of Mt. Etna volcanic plume retrieved by means of the Airborne Multispectral Imaging Spectrometer MIVIS. *Annals of Geophysics*, 46 (2).
- Spinetti, C. Buongiorno, M.F. Volcanic water vapour abundance retrieved using hyperspectral data *Geoscience and Remote Sensing Symposium, IGARSS '04. Proceedings.* (2004) 2004 IEEE International Publication Date: 20-24 Sept. 2004 Volume: 2, On page(s): 1487- 1490 vol.2
- Synthetic Aperture Radar Computer Compatible Tape Format Specifications", (CEOS SAR CCT Iss/Rev: 2/1) by CEOS WGD on SAR data Standards, March 1989, revision 1 January 1992
- Teggi. S., Bogliolo MP, Buongiorno MF, Pugnaghi S., Sterni A. (1999), Evaluation of SO<sub>2</sub> emission from Mount Etna using diurnal and nocturnal IR and visibile imaging spectrometer thermal IR remote sensing images and radiative transfer models, *Journal of Geophysical Research*, vol. 104, n. B9, pp. 20069-20079
- Tizzani, P., P. Berardino, F. Casu, P. Euillades, M. Manzo, G. P. Ricciardi, G. Zeni and R. Lanari (2007), Surface deformation of Long Valley caldera and Mono Basin, California, investigated with the SBAS-InSAR approach, *Remote Sensing of Environment*, doi: 10.1016/j.rse.2006.11.015e.
- Vermote E., D. Tanre', J. L. Deuze', M. Herman, and J. J. Morcrette.( 1997) "Second simulation of the satellite signal in the solar spectrum, 6S: an overview," *IEEE Trans. Geosci. Remote Sens.* 35, pp. 675-686
- Wen S., W. I. Rose, (1994) "Retrieval of sizes and total masses of particles in volcanic clouds using AVHRR bands 4 and 5", *J. of Geoph. Res.*, 99, D3, 5421-5431
- Wright R., Rothery, D.A., Blake, S., Pieri, D.C., (2000). Improved remote sensing estimates of lava flow cooling: a case study of the 1991-1993 Mount Etna eruption, *Journal of Geophysical Research*, 105, B10, 23,681-23,694.
- Zebker, H.A. Goldstein, R.M. (1986) Topographic mapping from interferometric SAR observations, *J. Geophys. Res.*, 91 4993- 5001.



## **Risk Management in Environment, Production and Economy**

Edited by Dr. Matteo Savino

ISBN 978-953-307-313-2

Hard cover, 214 pages

**Publisher** InTech

**Published online** 12, September, 2011

**Published in print edition** September, 2011

The term "risk" is very often associated with negative meanings. However, in most cases, many opportunities can present themselves to deal with the events and to develop new solutions which can convert a possible danger to an unforeseen, positive event. This book is a structured collection of papers dealing with the subject and stressing the importance of a relevant issue such as risk management. The aim is to present the problem in various fields of application of risk management theories, highlighting the approaches which can be found in literature.

### **How to reference**

In order to correctly reference this scholarly work, feel free to copy and paste the following:

Massimo Musacchio, Malvina Silvestri, Luca Merucci, Stefano Corradini, Claudia Spinetti, Valerio Lombardo, Boris Behncke, Lorenzo Guerrieri, Gabriele Gangale, Fabrizia Buongiorno, Sergio Perelli, Sergio Teggi, Sergio Pugnaghi, Angelo Amodio, Eugenio Sansosti, Simona Zoffoli and Chiara Cardaci (2011). Generation of Added Values Products Supporting Risk Analysis, Risk Management in Environment, Production and Economy, Dr. Matteo Savino (Ed.), ISBN: 978-953-307-313-2, InTech, Available from: <http://www.intechopen.com/books/risk-management-in-environment-production-and-economy/generation-of-added-values-products-supporting-risk-analysis>

# **INTech**

open science | open minds

### **InTech Europe**

University Campus STeP Ri  
Slavka Krautzeka 83/A  
51000 Rijeka, Croatia  
Phone: +385 (51) 770 447  
Fax: +385 (51) 686 166  
[www.intechopen.com](http://www.intechopen.com)

### **InTech China**

Unit 405, Office Block, Hotel Equatorial Shanghai  
No.65, Yan An Road (West), Shanghai, 200040, China  
中国上海市延安西路65号上海国际贵都大饭店办公楼405单元  
Phone: +86-21-62489820  
Fax: +86-21-62489821

© 2011 The Author(s). Licensee IntechOpen. This chapter is distributed under the terms of the [Creative Commons Attribution-NonCommercial-ShareAlike-3.0 License](#), which permits use, distribution and reproduction for non-commercial purposes, provided the original is properly cited and derivative works building on this content are distributed under the same license.